

Dopamine neurons release transmitter via a flickering fusion pore

Roland G W Staal, Eugene V Mosharov & David Sulzer^{1–3}

A key question in understanding mechanisms of neurotransmitter release is whether the fusion pore of a synaptic vesicle regulates the amount of transmitter released during exocytosis. We measured dopamine release from small synaptic vesicles of rat cultured ventral midbrain neurons using carbon fiber amperometry. Our data indicate that small synaptic vesicle fusion pores flicker either once or multiple times in rapid succession, with each flicker releasing ~25–30% of vesicular dopamine. The incidence of events with multiple flickers was reciprocally regulated by phorbol esters and staurosporine. Thus, dopamine neurons regulate the amount of neurotransmitter released by small synaptic vesicles by controlling the number of fusion pore flickers per exocytotic event. This mode of exocytosis is a potential mechanism whereby neurons can rapidly reuse vesicles without undergoing the comparatively slow process of recycling.

Several studies suggest that small synaptic vesicles (SSVs) release neurotransmitter by full fusion as well as through transient fusion pores ('kiss-and-run' exocytosis)^{1–3}. Capacitance recordings that monitor changes in plasma membrane surface area indicate that SSV endocytosis at the calyx of Held occurs 50–100 ms after fusion⁴ and that 5% of fusion events by pituitary SSV-like microvesicles are followed (within 2 s) by endocytosis⁵. These relatively rapid instances of vesicle endocytosis are consistent with formation of transient fusion pores. In the neuromuscular junction, the kinase inhibitor staurosporine attenuates the release of the amphipathic fluorescent dye FM1-43 more than the release of acetylcholine during SSV fusion⁶. This suggests that PKC inhibition reduces the SSV fusion pore aperture and may inhibit full fusion. In hippocampal neurons, kiss-and-run, full fusion and an intermediate mode of endocytosis can be observed by labeling SSVs with a pH-sensitive fluorescent protein⁷. Also in some hippocampal neurons, some SSV fusion events result in partial loss of FM1-43 fluorescence⁸, suggesting that the vesicles close before FM1-43 release is complete. Neurotransmitters, however, have far higher diffusion coefficients than FM1-43 (refs. 6,9), and it is not known whether transient pore openings are sufficient for release of the entire neurotransmitter content of an SSV. In addition, the kinetics of kiss-and-run exocytosis cannot be determined due to the insufficient temporal resolution of current approaches. We therefore adapted carbon fiber amperometry to record dopamine release from synaptic terminals of cultured rat ventral tegmental area neurons. This technique directly measures dopamine flux with a time resolution that is 2–5 orders of magnitude greater than capacitance, imaging and postsynaptic recordings (Methods). We found that small synaptic vesicles regulate the release of neurotransmitter via rapid flickering of the fusion pore.

RESULTS

Dopamine release from midbrain neurons

SSVs are the predominant synaptic vesicles in cultured dopamine neurons from the ventral midbrain of rats (>99%)^{10,11}. Neurons were stimulated with either 40 mM K⁺ (Fig. 1a) or a combination of 80 mM K⁺ and 20 nM α -latrotoxin (K⁺/ α -LTX; Fig. 1b). α -Latrotoxin inserts into the plasma membrane in a manner facilitated by neurexin-1 and CIRL/latrophilin receptors and forms a cation channel that enables Ca²⁺ to enter the cell, thereby increasing the number of exocytotic events¹² (Table 1 legend¹⁰).

Both secretagogues elicited a variety of amperometric peaks (Fig. 1c,d). The average number of dopamine molecules recorded per amperometric event was similar for both secretagogues (K⁺, 15,800 \pm 4,000 molecules; K⁺/ α -LTX, 11,600 \pm 1,700 molecules, $P > 0.1$), although events obtained by K⁺/ α -LTX stimulation had smaller amplitudes (maximum current; I_{\max}) (K⁺, 35.4 \pm 3.4 pA; K⁺/ α -LTX, 18.4 \pm 2.5 pA, $P < 0.05$, Mann-Whitney U -test) and increased durations (width at half-height; $t_{1/2}$) (K⁺, 108 \pm 12 μ s; K⁺/ α -LTX, 178 \pm 29 μ s, $P < 0.05$).

Simple and complex amperometric events

The shapes of 80–85% of amperometric events induced by either secretagogue closely resembled those previously reported for dopamine and serotonin release during SSV exocytosis^{10,11,13,14} (Fig. 1c). Such peaks, which we refer to as 'simple' events, consisted of a single rising and a single falling phase (Fig. 1e; Methods). Our random walk simulations of dopamine release indicated that the minimum fusion pore diameter consistent with the flux of dopamine observed in simple events was 1.5–3.5 nm (Methods). Surprisingly, this calculated diameter of the fusion pore in dopaminergic SSVs is nearly identical to estimates of the initial

Departments of ¹Neurology and ²Psychiatry, Black 305, 650 West 168th St, Columbia University, New York, New York 10032, USA. ³Department of Neuroscience, New York State Psychiatric Institute, 722 West 168th Street, New York, New York 10032, USA. Correspondence should be addressed to D.S. (ds43@columbia.edu).

Published online 29 February 2004; doi:10.1038/nn1205

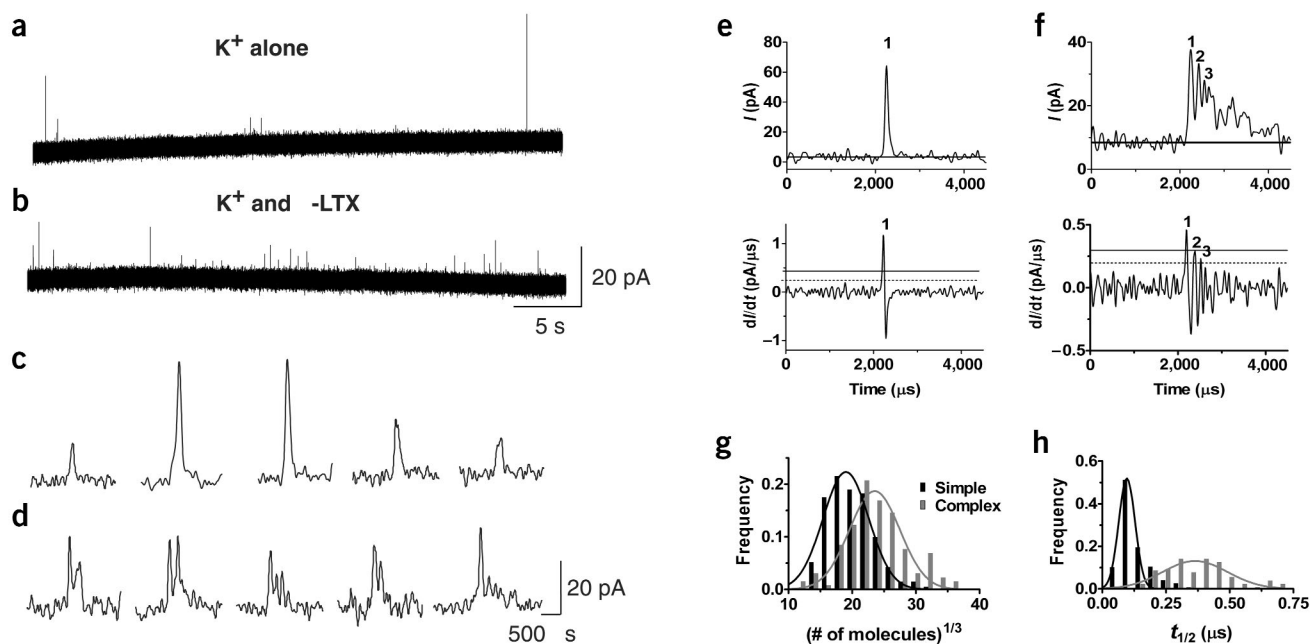


Figure 1 Dopamine release from axonal varicosities of rat ventral midbrain dopamine neurons. (a,b) Representative segment of current trace showing dopamine release from neurons stimulated with K^+ alone (a) or with K^+/α -LTX (b). The stimulus was given earlier in a portion of the trace that has been omitted because of the paucity of events. (c,d) Representative examples of simple events (c) and complex events (d). Simple events each have a single rising and falling slope, whereas complex events have multiple flickers, each with distinct rising and falling phases (Methods). (e,f) The upper panels show examples of amperometric current traces; the lower panels show the first derivative (dI/dt) of the currents. In the amperometric traces, the mean background current is indicated by a solid line (upper panel). To be considered an 'event,' the dI/dt must cross a $4.5 \times$ r.m.s. threshold (solid line, lower panel). (e) Events with derivatives that cross the $3.0 \times$ r.m.s. threshold (dotted line) only once in a rising trajectory are 'simple'. (f) Events that cross the $3.0 \times$ r.m.s. threshold multiple times are 'complex'. The corresponding flickers (1–3) are indicated in the current trace. (g,h) Histograms of simple versus complex event characteristics obtained from amperometric recordings after K^+/α -LTX stimulation ($n = 532$ simple events and $n = 130$ complex events from eight sites; see Table 1 for statistics).

fusion pore formed by large dense-core vesicles (LDCVs) in eosinophils, neutrophils and chromaffin cells^{15–17} even though the volume of LDCVs is 3–4 orders of magnitude larger.

The remaining events, which we refer to as 'complex' events (Fig. 1d), contained multiple, well-defined rising and falling phases (Fig. 1f; see Methods for flicker detection protocol). Complex events consisted of 2–5 'flickers' that occurred at a mean frequency of ~ 4 kHz (Table 1) and decreased in amplitude from the first to the last flicker (Table 2 and Fig. 2a). Complex events also showed significantly longer durations and released a greater number of molecules than simple events ($P < 0.05$; Fig. 1g,h and Table 1). As durations of consecutive flickers did not increase (Table 2), both the distance between the site of release and the recording electrode, and the diameter and open time of the fusion pore, were apparently unchanged.

Pharmacological regulation of events

Previous studies have suggested that phorbol esters can increase the number of secretory events via activation of Munc-13 (refs. 18,19). In addition, they can enhance the calcium sensitivity of transmitter release^{20,21} and modulate the kinetics of fusion pore formation^{22,23} via protein kinase C (PKC). The nonspecific kinase inhibitor staurosporine is reported to promote kiss-and-run exocytosis, possibly through inhibition of PKC^{6,24}.

We found that phorbol 12,13-dibutyrate (PDBU; $3 \mu\text{M}$, 15–30 min) increased the total number of exocytotic events per stimulus (Table 1 legend), consistent with the ability of phorbol esters to increase the size of the readily releasable pool of SSVs^{17,18,25}. In the presence of staurosporine ($5 \mu\text{M}$, 15–30 min), fewer amperometric events were recorded upon stimulation with K^+/α -LTX, and no events were detected when K^+ alone was applied. PDBU decreased the

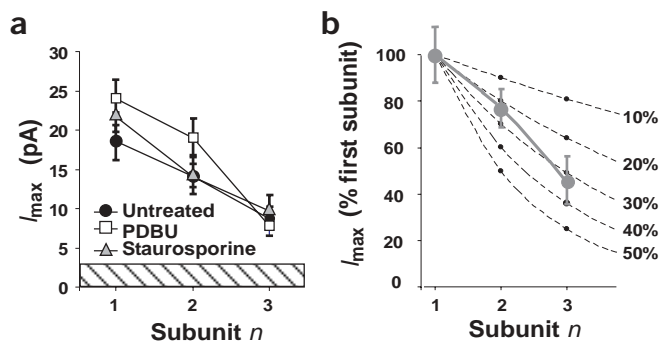


Figure 2 Amplitudes of flickers within complex events. (a) The amplitude (mean \pm s.e.m.) of each flicker (I_{max}) is plotted against the flicker n . Only flickers from complex events with an $I_{\text{max}} > 20$ pA are shown because of the increased contribution of background noise to smaller flickers (~ 3 pA r.m.s., hatched box; $n = 21$ complex events for untreated, 23 for PDBU-treated and 9 for staurosporine-treated; all were K^+/α -LTX-stimulated events). (b) Dependence of flicker I_{max} on the fraction of total neurotransmitter released per pore opening. The mean values of the experimental data from untreated neurons (solid line, gray circles) yielded a slope of -4.7 ± 1.7 pA/flicker (mean \pm s.d.), corresponding to the decrease predicted for release of $26 \pm 9\%$ of transmitter content (mean \pm s.d.; $r^2 = 0.97$).

Table 1 Characteristics of simple and complex events elicited by K⁺ and K⁺/α-LTX

Simple events					
	Number of dopamine molecules	I_{\max} (pA)	$t_{1/2}$ (μs)		
K ⁺ control	10,400 ± 1,000	35.2 ± 3.3	92 ± 6		
PDBU	8,300 ± 1,100	30.3 ± 2.9	76 ± 6*		
K ⁺ /α-LTX control	10,200 ± 1,500	17.7 ± 2.3	156 ± 30		
Staurosporine	14,000 ± 1,900	26.1 ± 5.1	164 ± 38		
PDBU	8,200 ± 1,000	25.7 ± 4.4	91 ± 4		
Complex events					
	Number of dopamine molecules	I_{\max} (pA)	$t_{1/2}^{\text{complex}}$ (μs)	Inter-flicker interval (μs)	Flickers/event
K ⁺ control	23,700 ± 8,000‡	26.9 ± 4.8	380 ± 43‡	240 ± 27	2.06 ± 0.06
PDBU	25,800 ± 6,400*‡	26.4 ± 2.2	461 ± 83‡	293 ± 71	2.38 ± 0.22
K ⁺ /α-LTX control	18,200 ± 4,900‡	20.2 ± 4.2	507 ± 48‡	261 ± 46	2.32 ± 0.03
Staurosporine	26,400 ± 5,500‡	33.2 ± 6.4	573 ± 61‡	322 ± 24*	2.51 ± 0.19
PDBU	14,200 ± 2,300‡	19.1 ± 3.2	291 ± 41**‡	165 ± 28**	2.19 ± 0.12

For K⁺-stimulated neurons, the data are presented from untreated neurons (8 sites, 13 ± 4 events per site; mean ± s.e.m.) and PDBU-treated neurons (7 sites, 77 ± 56 events per site). No events were detected from neurons treated with staurosporine when K⁺ alone was used as a secretagogue. For K⁺/α-LTX-stimulated neurons, the data are presented from untreated (8 sites, 85 ± 50 events per site), staurosporine-treated (11 sites, 15 ± 7 events per site) and PDBU-treated neurons (9 sites, 94 ± 41 events per site). Data in the table are shown as mean ± s.e.m. for each recording site: **P* < 0.05 and ***P* < 0.005 for PDBU or staurosporine versus control, †*P* < 0.05 for PDBU versus staurosporine, ‡*P* < 0.05 for complex versus simple events by two-way ANOVA. Inter-flicker intervals are shown for complex events with I_{\max} > 20 pA.

incidence of complex events from 15% to 10% (K⁺ alone) and from 20% to 6% (K⁺/α-LTX, Fig. 3), whereas staurosporine doubled the incidence of complex events to 40% (K⁺/α-LTX). The number of flickers per complex event did not significantly change according to treatment or secretagogue used (Table 1).

DISCUSSION

Over a decade ago, the amperometric detection of catecholamines released during exocytosis was first applied to chromaffin cells that contain LDCVs²⁶. Subsequent studies used amperometry to detect neurotransmitter release from SSVs in neuronal cell bodies^{13,14,27,28} and central synaptic terminals¹⁰. Our measurements of dopamine released from terminals of cultured midbrain neurons show at least two types of amperometric events, which we labeled simple and complex. In contrast to simple events, which consisted of single amperometric peaks, complex events comprised 2–5 flickers that decreased sequentially in amplitude. Although it has long been remarked that exocytosis is not always an all-or-none event²⁹, flickers have not been previously described for SSV exocytosis because other recording techniques do not provide sufficient time resolution to resolve flickers within complex events.

Mechanisms of SSV exocytosis

In Figure 4, we illustrate several possible mechanisms of exocytosis that could produce complex events. One scenario is that two or more SSVs may release their contents simultaneously, but at different distances from the recording electrode, thus producing overlapping simple events (Fig. 4a). Such an overlap would need to be well coordinated, as the incidence of complex events in untreated neurons was 200-fold greater than the probability that any two simple events would occur randomly within the duration of a complex event (Methods). In addition, the apparent duration of the events released farther from the electrode would be longer as a result of diffusional filtering (that is, $t_{1/2}$ of flicker 1 ≠ $t_{1/2}$ of flicker 2). Alternatively, an

overlap of simple events could be due to the fusion of clustered SSVs where exocytosis of a single vesicle within a cluster would trigger the fusion of other vesicles (Fig. 4b). In this case, the average I_{\max} for flickers within complex events would be identical regardless of order (that is, I_{\max} of flicker 1 = I_{\max} of flicker 2). In a variation of this model, exocytosis could occur via the fusion of an SSV to another SSV that had already fused with the plasma membrane (Fig. 4c); in this case, later flickers would show an increased duration as a result of diffusional filtering and the dilution of neurotransmitter inside the two fused vesicles. As has been demonstrated for LDCVs³⁰, multiple SSVs might fuse with each other before exocytosis, allowing the vesicle contents to mix (compound exocytosis). The resulting vesicle would either produce a single peak or, if the SSV matrices or cores remained intact after SSVs fusion, multiple peaks with similar amplitudes and durations (Fig. 4d). All of the above hypotheses were contradicted by our experimentally determined I_{\max} and $t_{1/2}$ values of complex event flickers, which decreased sequentially (Fig. 2a and Table 2).

In contrast to the above models of multiple SSV fusion, complex events could result from the fusion of a single SSV that forms a rapidly flickering fusion pore (Fig. 4e). In this case, the I_{\max} of each subsequent flicker would decrease because of the reduced SSV neurotransmitter concentration after each pore opening (I_{\max} of flicker 1 > I_{\max} of flicker 2). This hypothesis was supported by the observed decrease in the average I_{\max} of successive flickers within complex events (Fig. 2a and Table 2), which corresponded to the release of ~25–30% of the SSV neurotransmitter content per flicker for neurons in all treatment groups (Fig. 2b). The slight decrease in the $t_{1/2}$ of flickers within complex events (Table 2) is consistent with random walk simulations, suggesting that this decrease is due to the filtering applied to the data (data not shown).

Although some studies show transient flickering of the fusion pore in LDCVs^{31,32}, the duration of SSV flickers observed here was considerably shorter than reported for LDCVs (100–150 μs vs.

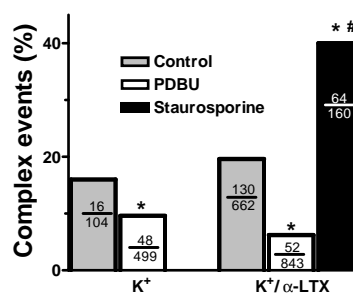


Figure 3 Pharmacological regulation of the incidence of complex events. The percentages of complex events are shown for each experimental condition. The numbers of complex events/total number of events are indicated within the bars. **P* < 0.05 vs. control, #*P* < 0.005 vs. PDBU, by chi-square test. No events were detected after K⁺ stimulation of staurosporine-treated neurons.

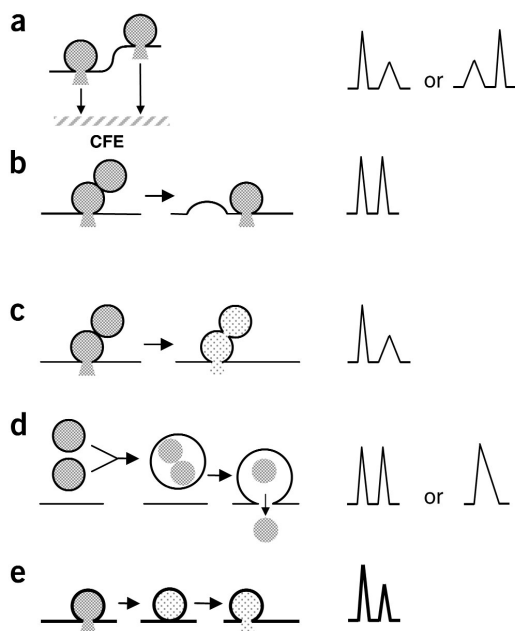


Figure 4 Mechanisms that may explain complex events (left column) and predicted averaged amperometric event shape (right column). (a) Overlap of simple events with spatial separation of release sites. Either vesicle could release first, resulting in either of the scenarios depicted on the right. The carbon fiber electrode (CFE) is 100 times wider than the diameter of the SSVs, and has been omitted in b–e. (b) Exocytosis of clustered vesicles. (c) Vesicle fusion with another vesicle that has already fused to the membrane. (d) If the vesicular matrices remain intact, compound exocytosis would occur without mixing of vesicular contents. If the matrices are labile, the contents would mix, resulting in a single amperometric peak. (e) Transmitter release from a single SSV via a flickering fusion pore.

10,000–500,000 μs , respectively). We also found that they occurred at a much higher frequency than in LDCVs (4,000 Hz vs. 170 Hz)³² and released a far greater fraction of the vesicle's neurotransmitter (25–30% vs. <1%)³².

Relevance to vesicle recycling

For all treatment groups, the number of molecules in complex amperometric events was significantly greater than in simple events (1.7–3.1 fold; $P > 0.05$; Table 1 and Fig. 1g). Interestingly, the first flicker within complex events was similar to simple events in amplitude (18.4 ± 2.2 vs. 17.7 ± 2.3 pA), number of molecules ($10,800 \pm 800$ vs. $10,200 \pm 1,500$ molecules) and $t_{1/2}$ (129 ± 13 vs. 156 ± 30 μs ; Tables 1 and 2). These data suggest that simple events may generally represent neurotransmitter release through short-lived pores that are not open long enough to release an SSV's entire neurotransmitter content, implying kiss-and-run exocytosis. Complex events appear to be exocytotic events in which the fusion pore either flickers (opens and closes) or fluctuates (enlarges and constricts) several times in rapid succession, resulting in the release of a larger fraction of an SSV's neuro-

Table 2 Characteristics of complex event flickers

Flicker	Number of dopamine molecules	I_{max} (pA)	$t_{1/2}$ (μs)
1 st	$10,800 \pm 800$	18.4 ± 2.2	129 ± 13
2 nd	$7,500 \pm 1,200^*$	$14.2 \pm 1.5^*$	110 ± 9
3 rd	$6,000 \pm 2,400^*$	$8.4 \pm 1.9^{\dagger*}$	$91 \pm 8^*$

Data are for flickers 1–3 from complex events with $I_{\text{max}} > 20$ pA in untreated neurons stimulated with $\text{K}^+/\text{a-LTX}$ (mean \pm s.e.m.). * $P < 0.05$ compared with 1st flicker and $\dagger P < 0.05$ compared with 2nd flicker.

transmitter content. Whereas full fusion of SSVs has been clearly demonstrated³³, data from the present study and others^{7,8} suggest that some synapses primarily use kiss-and-run exocytosis. The presynaptic terminals of midbrain dopamine neurons contain a relatively small number of SSVs³⁴ with an apparently high probability of exocytosis for any given vesicle³⁵. Fusion pore flickering and kiss-and-run exocytosis may be particularly important for such synapses to prevent the loss of SSVs during full fusion and the relatively slow process of endocytosis and recycling.

Relevance for dopamine signaling

In contrast to fast-acting neurotransmitter systems with well-defined pre- and postsynaptic structures, dopamine neurons form 'social' synapses that often lack well-defined active zones^{35–38}. The dopamine reuptake transporters are located some distance away from the release site, enabling the neurotransmitter to diffuse and act on receptors several microns away^{37,38}. Modeling of the diffusion of dopamine released at social synapses in the striatum suggests that the number of molecules released per exocytotic event (quantal size) determines how far dopamine diffuses and how many receptors are activated^{37–39}. Because the number of molecules released during complex events is greater than in simple events, dopamine will diffuse through a larger volume (Fig. 5a,b), activating more receptors for a longer duration (Fig. 5c).

In summary, our data provide evidence that second-messenger systems modulate the mode of SSV exocytosis by regulating the number of fusion pore flickers per exocytotic event. Fusion pore flickering may provide neurons with a means to recycle vesicles more efficiently and to control quantal size, thus regulating the spillover of neurotransmitter from a social synapse.

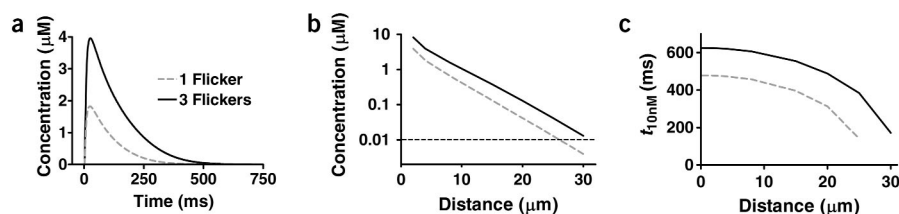


Figure 5 Simulated dopamine spillover in the striatum. (a) Diffusion profiles of dopamine released from an SSV following one or three openings of the fusion pore (10,000 and 20,000 dopamine molecules released, respectively; Table 1) at $4 \mu\text{m}$ from the release site as determined by random walk simulations. (b) Maximum dopamine concentrations reached at various distances from the release site. The straight dashed line at 10 nM indicates the EC_{50} for the activation of dopamine receptors (1–20 nM)⁴⁸. (c) The duration that receptors are exposed to dopamine levels > 10 nM. Dopamine spillover from a single flicker activates receptors in a $73,500 \mu\text{m}^3$ sphere (26 μm radius), with nearby receptors activated for 480 ms. If the SSV flickers three times, then the volume of the sphere is 1.7-fold larger ($\sim 125,000 \mu\text{m}^3$, 31 μm radius) and the duration of receptor activation is 620 ms. These calculations are based on vesicular dopamine concentrations in L-DOPA pretreated neurons, which are 3–5 fold higher than in untreated cultures¹⁰.

METHODS

Rat ventral midbrain neuronal cultures. Postnatally derived ventral midbrain neurons were cultured as previously described⁴⁰. Neurons were preincubated with 100 μ M L-DOPA for 30 min prior to recording¹¹. The secretagogues (92 mM NaCl, 40 mM KCl, 10 mM HEPES, 1 mM Na₂HPO₄, 2 mM MgCl₂, 1.2 mM CaCl₂, ~300 mosm and pH 7.4 or 52 mM NaCl, 80 mM KCl, 10 mM HEPES, 1 mM Na₂HPO₄, 2 mM MgCl₂, 1.2 mM CaCl₂ and 20 nM α -LTX) were applied by local perfusion through a glass micropipette (Picospritzer, General Valve) for 6 s at 10 p.s.i. and ~30 μ m from the recording site.

Amperometric recordings. A 5- μ m diameter carbon fiber electrode held at +700 mV was positioned over a potential release site (Newport micromanipulator MX300R) and lowered until the tissue was slightly depressed¹⁰. At this potential, dopamine is oxidized, resulting in the donation of two electrons to the electrode. Thus, the number of molecules reaching the electrode can be estimated from the current³⁸. The current was filtered using a 4-pole 10 kHz Bessel filter built into an Axopatch 200A amplifier (Axon Instruments), sampled at 100 kHz (PCI-6052E, National Instruments) and digitally filtered using a binomial 10 routine (Igor Pro, Wave Metrics) with a -3 dB cut-off of ~15 kHz. This yielded an overall -3 dB cut-off frequency of >8 kHz and essentially no time distortion for the $t_{1/2}$ of amperometric events with durations >50 μ s. It also broadened events of shorter duration toward 50 μ s⁴¹. Traces with root mean square (r.m.s.) noise less than 3 pA r.m.s. were analyzed. The background noise was normally distributed with no maxima for any frequency component between 0.6 and 33 kHz. No events were recorded when the applied voltage was adjusted to 0 mV or when the electrode was transiently lifted from an active recording site.

Peak detection and flicker analysis. Raw amperometric data were collected and analyzed using a locally written routine in Igor Pro. The first derivative of the current trace (dI/dt) was used to detect amperometric events. The r.m.s. of the dI/dt noise was first measured in a segment of the trace that did not contain peaks. Then, dI/dt was used to detect events that were 4.5-fold larger than the r.m.s. noise. These spikes represented the total population of amperometric events. The beginning and the maximum of each event were at $dI/dt = 0$ (Fig. 1e,f). The end of an event was defined as the point when the current returned to the baseline value. If there was more than one maximum within an event and the dI/dt of these maxima (flickers) was three-fold larger than the r.m.s. noise, then the event was classified as 'complex' (Fig. 1f). Events that included a single peak with one rising and one falling phase or for which the dI/dt of flickers was less than three times the r.m.s. noise were categorized as 'simple' events. This approach was relatively conservative in identifying flickers, but the same rules were applied for each treatment. We found that the same flickers were identified independently of their order within a complex event.

Due to the shape of complex events, the typical $t_{1/2}$ value does not accurately reflect the event's duration. Thus, the duration of complex events was calculated as:

$$t_{1/2}^{\text{complex}} = \frac{(t(f_n) - t(f_1) + t_{1/2}(f_1) + t_{1/2}(f_n))}{2} \quad (1)$$

where $t(f_1)$ and $t(f_n)$ are the times at I_{max} , and $t_{1/2}(f_1)$ and $t_{1/2}(f_n)$ are the durations of the first and the last flickers of complex events. The number of molecules in the first flicker was estimated by subtracting the integral of the subsequent flickers from the integral of the entire complex event. The baseline for the subsequent flickers was estimated as a line from the beginning of the second event to the end of the complex event. Although this approach may slightly overestimate the number of molecules in the first flicker as a result of the nonlinear decay of events, this error would be <2%.

Statistical analysis. The data in Table 1 are reported as averages of the mean values from each recording site⁴², each of which generally represents a single presynaptic terminal¹⁰. Data were analyzed by ANOVA of the means unless indicated otherwise⁴². As reported in several studies, the numbers of mole-

cules (n) released during exocytotic events are distributed as a function of vesicle volumes so that the cube roots of n result in a normal distribution (Fig. 1g; for review, see ref. 38). As previously reported¹⁰, occasional large events (3 of 772 in untreated cultures) were >5 standard deviations greater than the geometric mean of the cube roots of n and were excluded from the data analysis in Table 1. The data in Figure 4 are nonparametric and were analyzed by chi-square test.

Estimation of the expected random overlap of simple events. The probability that complex events resulted from the random overlap of simple events can be estimated from the exponential decay of interspike intervals³⁸. The time constant was 545 ms ($R^2 = 0.997$ from untreated cultures; Supplementary Fig. 1 online). The probability of observing an interspike interval less than 0.5 ms (two overlapping events within the duration of complex events) is $P = (1 - e^{-0.5/545}) \times 100 = 0.09\%$.

Simulation of dopamine release from the vesicle. Random walk simulations³⁸ (finite-difference model) of molecular diffusion to an amperometric ('consuming') electrode was performed using Excel software (Microsoft). During each time bin (t_{bin}), the flux (J , molecules/s) of dopamine molecules from the vesicle through a fusion pore was calculated as:

$$J = \frac{a \cdot C_v \cdot D}{b} = \frac{\pi \cdot (R_{\text{pore}} [\text{cm}])^2 \cdot \frac{N_v [\text{molecules}]}{\frac{4}{3} \pi \cdot (R_v [\text{cm}])^3} \cdot D [\text{cm}^2/\text{s}]}{b [\text{cm}]} \quad (2)$$

where a is the area, b is the length and R_{pore} is the radius of a cylindrical pore⁴³. C_v and N_v are the concentration and the number of molecules of neurotransmitter in the vesicle with radius R_v . D is the diffusion coefficient, which is 6.9×10^{-6} cm²/s for dopamine in aqueous solution⁴⁴. We used electron micrographs of tyrosine hydroxylase-immunolabeled cultures to determine SSV diameters under the conditions used in the recordings. SSV diameters were similar to those of previous reports¹¹; 50.7 ± 1.4 nm (mean \pm s.e.m., $n = 49$ vesicles in 7 terminals; data not shown). The length of the fusion pore was estimated as 7.5–15 nm, twice the membrane thickness of 5-hydroxydopamine-labeled SSVs in this preparation¹¹. The distance between the release site and electrode was varied from 50–400 nm, beyond which the amperometric currents would be too low in amplitude to be identified. The number of molecules (N) encountering the surface of the amperometric electrode during t_{bin} was converted to units of amperometric current (I) using the following formula³⁸:

$$I_{[\text{pA/s}]} = \frac{N [\text{molecules}] \cdot 10^6 [\mu\text{s}]}{t_{\text{bin}} [\mu\text{s}] \cdot 3.121 \cdot 10^6 [\text{molecules} \cdot \text{s/pA}]} \quad (3)$$

For simulations, the diameter and the length of the fusion pore as well as the number of molecules inside the vesicle were varied until the amplitude and duration of simulated exocytotic events (after resampling and filtering) were the same as the average $t_{1/2}$ and I_{max} of the amperometric peaks that had been recorded experimentally (Table 1). Simulated data were re-sampled at 10- μ s intervals and filtered using binomial 10 smoothing to mimic the experimental conditions.

Given that dopamine is present in high millimolar concentrations within the SSV, it is possible that dissociation of dopamine from a luminal core is slower than the diffusion of free molecules through the fusion pore. Additionally, the pore length may be longer than the thickness of the plasma membrane⁴⁵. Thus, the calculated pore diameters represent a minimum estimate.

Simulation of dopamine diffusion in striatum. Dopamine spillover was modeled using the diffusion coefficient of dopamine in the striatum, 2.7×10^{-6} cm²/s (ref. 46). The dopamine concentration next to the fusion pore was calculated as:

$$C_{[M]} = \frac{N[\text{molecules}] \cdot 6.022 \cdot 10^{23}[\text{molecules/mole}]}{\frac{4}{3} \pi \cdot (r_{\text{bin}}[\text{dm}])^3} \quad (4)$$

where r_{bin} is the radius of the sphere next to the fusion pore derived as $r_{\text{bin}} = \sqrt{(t_{\text{bin}}/2D)}$. Dopamine uptake via the dopamine transporter was assumed to follow Michaelis-Menten kinetics, with $V_{\text{max}} = 4.88 \mu\text{M/s}$ and $K_m = 0.77 \mu\text{M}$ (ref. 47).

A tutorial on random walk and finite difference simulations and the Excel spreadsheets used for these calculations are available at our laboratory website (http://www.columbia.edu/~ds43/pore_RW.html).

Note: Supplementary information is available on the Nature Neuroscience website.

ACKNOWLEDGMENTS

We thank Q. Al-Awqati, K. Larsen, M. Nirenberg and Y. Schmitz for critique of the manuscript, and A. Petrenko for α -latrotoxin. Supported by the National Alliance for Research on Schizophrenia and Depression, the Lowenstein Foundation, the Parkinson's Disease Foundation, the National Institute on Drug Abuse and the National Institute of Neurological Disorders and Stroke.

COMPETING INTERESTS STATEMENT

The authors declare that they have no competing financial interests.

Received 23 October 2003; accepted 27 January 2004

Published online at <http://www.nature.com/natureneuroscience/>

- Valtorta, F., Meldolesi, J. & Fesce, R. Synaptic vesicles: is kissing a matter of competence? *Trends Cell Biol.* **11**, 324–328 (2001).
- Heuser, J.E. & Reese, T.S. Evidence for recycling of synaptic vesicle membrane during transmitter release at the frog neuromuscular junction. *J. Cell Biol.* **57**, 315–344 (1973).
- Ceccarelli, B., Hurlbut, W.P. & Mauro, A. Turnover of transmitter and synaptic vesicles at the frog neuromuscular junction. *J. Cell Biol.* **57**, 499–524 (1973).
- Sun, J.Y., Wu, X.S. & Wu, L.G. Single and multiple vesicle fusion induce different rates of endocytosis at a central synapse. *Nature* **417**, 555–559 (2002).
- Klyachko, V.A. & Jackson, M.B. Capacitance steps and fusion pores of small and large-dense-core vesicles in nerve terminals. *Nature* **418**, 89–92 (2002).
- Henkel, A.W. & Betz, W.J. Staurosporine blocks evoked release of FM1-43 but not acetylcholine from frog motor nerve terminals. *J. Neurosci.* **15**, 8246–8258 (1995).
- Gandhi, S.P. & Stevens, C.F. Three modes of synaptic vesicular recycling revealed by single-vesicle imaging. *Nature* **423**, 607–613 (2003).
- Aravanis, A.M., Pyle, J.L. & Tsien, R.W. Single synaptic vesicles fusing transiently and successively without loss of identity. *Nature* **423**, 643–647 (2003).
- Stiles, J.R., Van Helden, D., Bartol, T.M. Jr., Salpeter, E.E. & Salpeter, M.M. Miniature endplate current rise times less than 100 microseconds from improved dual recordings can be modeled with passive acetylcholine diffusion from a synaptic vesicle. *Proc. Natl. Acad. Sci. USA* **93**, 5747–5752 (1996).
- Pothos, E.N., Davila, V. & Sulzer, D. Presynaptic recording of quanta from midbrain dopamine neurons and modulation of the quantal size. *J. Neurosci.* **18**, 4106–4118 (1998).
- Pothos, E.N. *et al.* Synaptic vesicle transporter expression regulates vesicle phenotype and quantal size. *J. Neurosci.* **20**, 7297–7306 (2000).
- Bittner, M.A. Alpha-latrotoxin and its receptors C1RL (latrophilin) and neurexin 1 alpha mediate effects on secretion through multiple mechanisms. *Biochimie* **82**, 447–452 (2000).
- Bruns, D. & Jahn, R. Real-time measurement of transmitter release from single synaptic vesicles. *Nature* **377**, 62–65 (1995).
- Hochstetler, S.E., Puopolo, M., Gustincich, S., Raviola, E. & Wightman, R.M. Real-time amperometric measurements of zeptomole quantities of dopamine released from neurons. *Anal. Chem.* **72**, 489–496 (2000).
- Hartmann, J., Sceppek, S. & Lindau, M. Regulation of granule size in human and horse eosinophils by number of fusion events among unit granules. *J. Physiol. (Lond.)* **483**, 201–209 (1995).
- Lollike, K., Borregaard, N. & Lindau, M. The exocytotic fusion pore of small granules has a conductance similar to an ion channel. *J. Cell Biol.* **129**, 99–104 (1995).
- Albillos, A. *et al.* The exocytic event in chromaffin cells revealed by patch amperometry. *Nature* **389**, 509–512 (1997).
- Betz, A. *et al.* Munc13-1 is a presynaptic phorbol ester receptor that enhances neurotransmitter release. *Neuron* **21**, 123–136 (1998).
- Rhee, J.S. *et al.* Beta phorbol ester- and diacylglycerol-induced augmentation of transmitter release is mediated by Munc13s and not by PKCs. *Cell* **108**, 121–133 (2002).
- Zhu, H., Hille, B. & Xu, T. Sensitization of regulated exocytosis by protein kinase C. *Proc. Natl. Acad. Sci. USA* **99**, 17055–17059 (2002).
- Yang, Y., Udayasankar, S., Dunning, J., Chen, P. & Gillis, K.D. A highly Ca^{2+} -sensitive pool of vesicles is regulated by protein kinase C in adrenal chromaffin cells. *Proc. Natl. Acad. Sci. USA* **99**, 17060–17065 (2002).
- Wang, P., Wang, C.T., Bai, J., Jackson, M.B. & Chapman, E.R. Mutations in the effector binding loops in the C2A and C2B domains of synaptotagmin I disrupt exocytosis in a nonadditive manner. *J. Biol. Chem.* **278**, 47030–47037 (2003).
- Graham, M.E., Fisher, R.J. & Burgoyne, R.D. Measurement of exocytosis by amperometry in adrenal chromaffin cells: effects of clostridial neurotoxins and activation of protein kinase C on fusion pore kinetics. *Biochimie* **82**, 469–479 (2000).
- Sceppek, S., Coorsen, J.R. & Lindau, M. Fusion pore expansion in horse eosinophils is modulated by Ca^{2+} and protein kinase C via distinct mechanisms. *EMBO J.* **17**, 4340–4345 (1998).
- Gillis, K.D., Mossner, R. & Neher, E. Protein kinase C enhances exocytosis from chromaffin cells by increasing the size of the readily releasable pool of secretory granules. *Neuron* **16**, 1209–1220 (1996).
- Wightman, R.M. *et al.* Temporally resolved catecholamine spikes correspond to single vesicle release from individual chromaffin cells. *Proc. Natl. Acad. Sci. USA* **88**, 10754–10758 (1991).
- Chen, G., Gavin, P.F., Luo, G. & Ewing, A.G. Observation and quantitation of exocytosis from the cell body of a fully developed neuron in *Planorbis corneus*. *J. Neurosci.* **15**, 7747–7755 (1995).
- Jaffe, E.H., Marty, A., Schulte, A. & Chow, R.H. Extrasynaptic vesicular transmitter release from the somata of substantia nigra neurons in rat midbrain slices. *J. Neurosci.* **18**, 3548–3553 (1998).
- Girod, R., Correges, P., Jacquet, J. & Dunant, Y. Space and time characteristics of transmitter release at the nerve-electrode junction of Torpedo. *J. Physiol.* **471**, 129–157 (1993).
- Hafez, I., Stolpe, A. & Lindau, M. Compound exocytosis and cumulative fusion in eosinophils. *J. Biol. Chem.* **278**, 44921–44928 (2003).
- Alvarez de Toledo, G., Fernandez-Chacon, R. & Fernandez, J.M. Release of secretory products during transient vesicle fusion. *Nature* **363**, 554–558 (1993).
- Zhou, Z., Mislser, S. & Chow, R.H. Rapid fluctuations in transmitter release from single vesicles in bovine adrenal chromaffin cells. *Biophys. J.* **70**, 1543–1552 (1996).
- Cremona, O. & De Camilli, P. Synaptic vesicle endocytosis. *Curr. Opin. Neurobiol.* **7**, 323 (1997).
- Pickel, V.M., Nirenberg, M.J. & Milner, T.A. Ultrastructural view of central catecholaminergic transmission: immunocytochemical localization of synthesizing enzymes, transporters and receptors. *J. Neurocytol.* **25**, 843–856 (1996).
- Garris, P.A., Ciolkowski, E.L., Pastore, P. & Wightman, R.M. Efflux of dopamine from the synaptic cleft in the nucleus accumbens of the rat brain. *J. Neurosci.* **14**, 6084–6093 (1994).
- Schmitz, Y., Benoit-Marand, M., Gonon, F. & Sulzer, D. Presynaptic plasticity of dopaminergic neurotransmission. *J. Neurochem.* **87**, 273–289 (2003).
- Gonon, F. *et al.* Geometry and kinetics of dopaminergic transmission in the rat striatum and in mice lacking the dopamine transporter. *Prog. Brain Res.* **125**, 291–302 (2000).
- Sulzer, D. & Pothos, E.N. Presynaptic mechanisms that regulate quantal size. *Rev. Neurosci.* **11**, 159–212 (2000).
- Cragg, S.J., Nicholson, C., Kume-Kick, J., Tao, L. & Rice, M.E. Dopamine-mediated volume transmission in midbrain is regulated by distinct extracellular geometry and uptake. *J. Neurophysiol.* **85**, 1761–1771 (2001).
- Pothos, E.N., Przedborski, S., Davila, V., Schmitz, Y. & Sulzer, D. D2-Like dopamine autoreceptor activation reduces quantal size in PC12 cells. *J. Neurosci.* **18**, 5575–5585 (1998).
- Colquhoun, D. & Sigworth, F.J. Fitting and statistical analysis of single-channel records. in *Single-Channel Recording* (eds. Sakmann, B. & Neher, E.) 483–587 (Plenum, New York, 1995).
- Colliver, T., Hess, E., Pothos, E.N., Sulzer, D. & Ewing, A.G. Quantitative and statistical analysis of the shape of amperometric spikes recorded from two populations of cells. *J. Neurochem.* **74**, 1086–1097 (1999).
- Berg, H.C. *Random Walks in Biology* 152 (Princeton Univ. Press, Princeton, 1983).
- Nicholson, C. Diffusion of ions and macromolecules in brain tissue. in *Monitoring Molecules in Neuroscience* Vol. 8 (eds. Røllme, H., Abercrombie, E., Sulzer, D. & Zackheim, J.) 71–73 (Rutgers Press, Newark, New Jersey, 1999).
- Jeremic, A., Kelly, M., Choo, S.J., Stromer, M.H. & Jena, B.P. Reconstituted fusion pore. *Biophys. J.* **85**, 2035–2043 (2003).
- Rice, M.E. *et al.* Direct monitoring of dopamine and 5-HT release in substantia nigra and ventral tegmental area *in vitro*. *Exp. Brain Res.* **100**, 395–406 (1994).
- Schmitz, Y., Lee, C.J., Schmauss, C., Gonon, F. & Sulzer, D. Amphetamine distorts synaptic dopamine overflow: effects on D2 autoreceptors, transporters, and synaptic vesicle stores. *J. Neurosci.* **21**, 5916–5924 (2001).
- Levant, B. The D3 dopamine receptor: neurobiology and potential clinical relevance. *Pharmacol. Rev.* **49**, 231–252 (1997).